

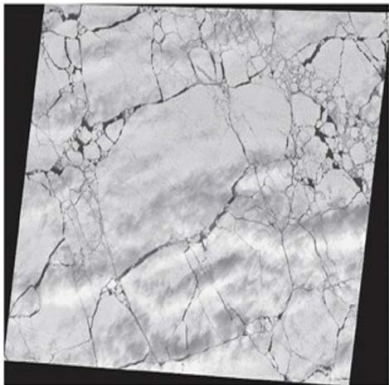
# Nonlinear waves in ice sheets

Philippe Guyenne

Department of Mathematical Sciences  
University of Delaware

Joint work with Emilian Părău (University of East Anglia, UK)

# Ice sheets



“Mathematics of Sea Ice Phenomena” (Isaac Newton Institute 2017)

- Motivation
- Mathematical formulation
- Hamiltonian equations
- Direct numerical simulation (**solitary waves**)
  - ▶ Steady solutions in a reference moving frame
  - ▶ Time-evolving solutions (stability?)
- Weakly nonlinear modeling
  - ▶ Modulational regime (**near  $k = k_0 > 0$** )
  - ▶ Long-wave/shallow-water regime (**near  $k = 0$** )

It is now recognized that ocean waves may have a significant impact on sea ice in polar regions

Expect to see ...

- weakened and more compliant sea ice because of warmer temperatures
- less compact sea ice
- larger ocean waves generated by more powerful storms
  - ▶ will penetrate further into the sea ice
  - ▶ have greater destructive payload to fracture the ice canopy
  - ▶ promote further melting by
    - ◇ breaking up the sea ice into smaller chunks
    - ◇ wave-induced melting

(e.g. Squire 2011; Thomson & Rogers 2014; Kohout et al. 2014)

# Sea ice and tsunamis



ESA/Envisat

March 2011 Tohoku tsunami caused large Manhattan-size icebergs to break off the Sulzberger Ice Shelf in Antarctica

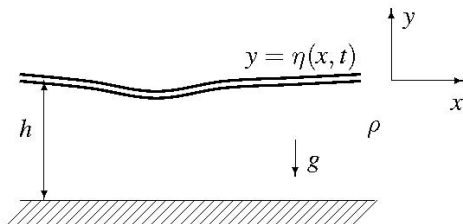
# Other applications: VLFS



Megafloat - Floating airport - Tokyo Bay

- Sea ice floes/sheets and compliant pontoon type VLFS are very similar in geometry and properties
- Same mathematical problems to be solved
- Climate change induced wave intensification important for both

## (2D) Governing equations



Incompressible, inviscid fluid and irrotational flow

$$\Delta\varphi = 0, \quad \text{for } -h < y < \eta$$

$$\partial_y\varphi = 0, \quad \text{on } y = -h$$

$$\partial_t\eta + \partial_x\eta \partial_x\varphi - \partial_y\varphi = 0, \quad \text{on } y = \eta \quad (\text{kinematic})$$

$$\partial_t\varphi + \frac{1}{2}|\nabla\varphi|^2 + g\eta + \frac{1}{\rho}P = 0, \quad \text{on } y = \eta \quad (\text{Bernoulli})$$

where  $P$  is the pressure exerted by the ice sheet on the fluid surface

# Model for the ice sheet

- Assumptions:
  - ▶ Thin elastic plate (ice thickness  $\ll$  wavelength)
  - ▶ Ice sheet bends in unison with ocean waves
  - ▶ No inertia, no stretching, only bending
  - ▶ Continuous ice sheet (no ice floes ... yet)
- The **linear** Euler–Bernoulli model

$$P = \mathcal{D} \partial_x^4 \eta, \quad \mathcal{D} = \text{coefficient of ice rigidity}$$

has been extensively used (Squire et al. 1996, etc.)

$$\mathcal{D} = \frac{\mathcal{E} \theta^3}{12(1 - \nu^2)}$$

where  $\theta$  is ice thickness,  $\mathcal{E} \approx 6$  GPa is Young's modulus and  $\nu \approx 0.3$  is Poisson's ratio



# Model for the ice sheet

- The (nonlinear) Kirchhoff–Love model

$$P = \mathcal{D} \partial_x^2 \left( \frac{\eta_{xx}}{(1 + \eta_x^2)^{3/2}} \right)$$

has also been used in a number of studies

- A more recent **nonlinear** model is given by the special Cosserat theory of hyperelastic shells (Plotnikov & Toland 2011)

$$P = \frac{\mathcal{D}}{\sqrt{1 + \eta_x^2}} \partial_x \left[ \frac{1}{\sqrt{1 + \eta_x^2}} \partial_x \left( \frac{\eta_{xx}}{(1 + \eta_x^2)^{3/2}} \right) \right] + \frac{\mathcal{D}}{2} \left( \frac{\eta_{xx}}{(1 + \eta_x^2)^{3/2}} \right)^3$$

where the term **in red** is the mean curvature at any point on the ice sheet.

# Model for the ice sheet

The Cosserat model has a number of interesting features:

- is highly nonlinear (suitable for large-amplitude ice deflections)
- satisfies Kirchhoff's hypothesis for elastic sheets
- conserves **elastic energy** (unlike Kirchhoff–Love)

$$E = \frac{1}{2} \int_{-\infty}^{\infty} \int_{-h}^{\eta} |\nabla\varphi|^2 dy dx + \frac{1}{2} \int_{-\infty}^{\infty} \left[ g\eta^2 + \frac{\mathcal{D}}{\rho} \frac{\eta_{xx}^2}{(1 + \eta_x^2)^{5/2}} \right] dx$$

- suggests a Hamiltonian formulation for nonlinear **ice-covered ocean waves** *à la Zakharov*
- has implications for asymptotics, numerics, etc.
- ... check out Walter and Onno's talks this week

For example ...

- Haragus-Courcelle & Ilichev (1998): Euler–Bernoulli, asymptotics
- Părău & Dias (2002): Love–Kirchhoff, asymptotics & numerics
- Hegarty & Squire (2008): Love–Kirchhoff, asymptotics & numerics
- Bonnefoy, Meylan & Ferrant (2009): Love–Kirchhoff, numerics
- Milewski, Vanden-Broeck & Wang (2011, 2013): Cosserat, asymptotics & numerics
- Guyenne & Părău (2012, 2014): Cosserat, asymptotics & numerics
- Ambrose & Siegel (2015?): Cosserat, analysis
- Groves, Hower & Wahlén (2016): Cosserat, analysis
- Dan Ratliff (soon?), Olga Trichtchenko (soon?), ...

# Hamiltonian formulation

Following Zakharov (1968) and Craig & Sulem (1993), define

$$\xi(x, t) = \varphi(x, \eta(x, t), t)$$

then the Hamiltonian equations are given by

$$\partial_t \begin{pmatrix} \eta \\ \xi \end{pmatrix} = \begin{pmatrix} 0 & 1 \\ -1 & 0 \end{pmatrix} \begin{pmatrix} \delta H / \delta \eta \\ \delta H / \delta \xi \end{pmatrix}$$

with Hamiltonian (i.e. energy)

$$H = \frac{1}{2} \int_{-\infty}^{\infty} \left[ \xi G(\eta) \xi + g\eta^2 + \frac{\mathcal{D}}{\rho} \frac{\eta_{xx}^2}{(1 + \eta_x^2)^{5/2}} \right] dx$$

where

$$G(\eta)\xi = (-\eta_x, 1)^\top \cdot \nabla \varphi \Big|_{y=\eta}$$

denotes the **Dirichlet–Neumann operator** (DNO) that returns the normal fluid velocity at the interface, given  $\eta$  and  $\xi$ .

# Waves induced by a moving load on sea ice

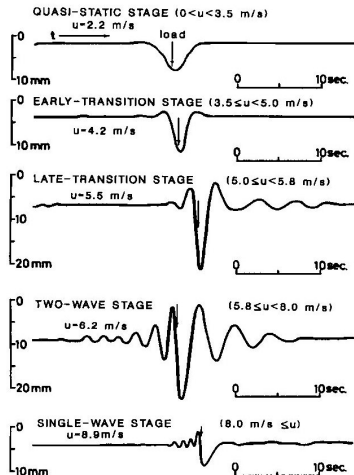


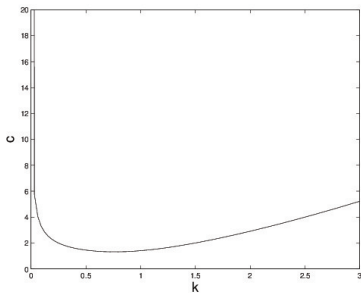
Fig. 1. Typical ice deflection records at various load speeds, February 5, 1981. (Reproduced by permission from Takizawa [1985].)

Experiments of Takizawa (1985) - Lake Saroma (Japan)

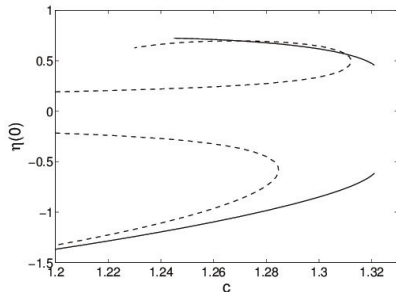
# Numerical results: branches of solutions

Linear dispersion relation: wave speed  $c$  vs. wavenumber  $k$

$$c^2 = \frac{g}{k} + \frac{\mathcal{D}k^3}{\rho} \quad \text{minimum at} \quad k_{\min} \approx 0.75, \quad c_{\min} \approx 1.32 \quad (h = \infty)$$



Linear dispersion relation

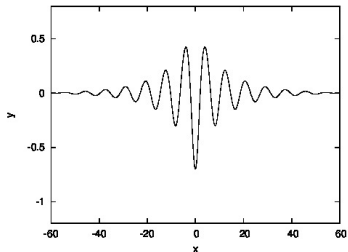


Nonlinear results

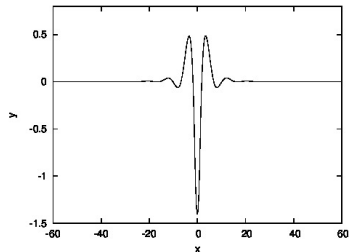
Free (solid line) and forced (dashed line) waves

Asymptotic regimes of interest: near  $k = 0$  and near  $k = k_{\min}$

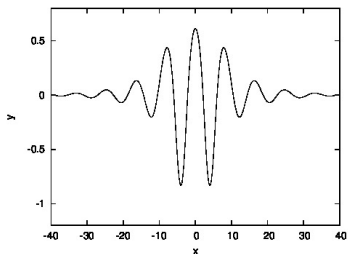
# Numerical results: wave profiles (BIE, $h = \infty$ )



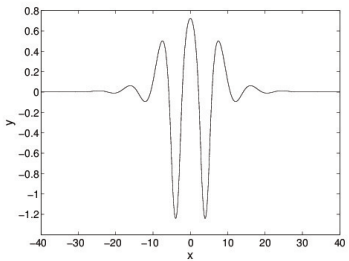
Solitary waves of depression  $c = 1.316$



$c = 1.192$



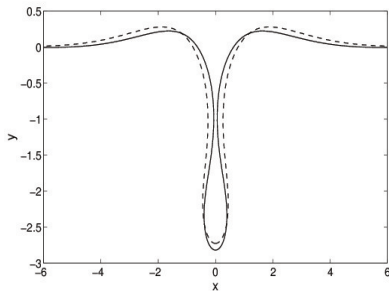
Solitary waves of elevation  $c = 1.301$



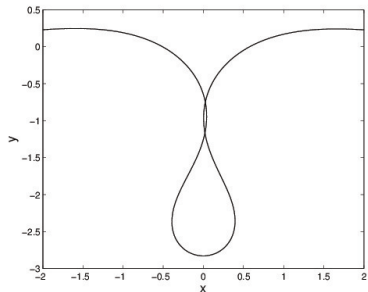
$c = 1.245$

# Numerical results: limiting profiles (BIE, $h = \infty$ )

Highly nonlinear solutions (as  $c \rightarrow 0$ ) ...



$c = 0.187$  (solid line) and  $c = 0.475$  (dashed line)

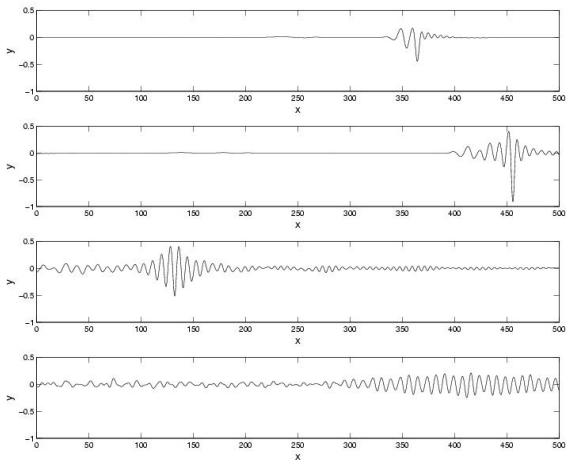


$c = 0$

Looks like Crapper's (bubble-shaped) solutions for capillary waves

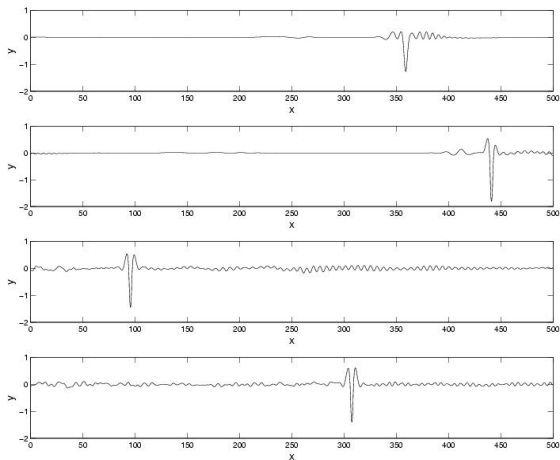


# Numerical results: stability (HOS, $h = \infty$ )



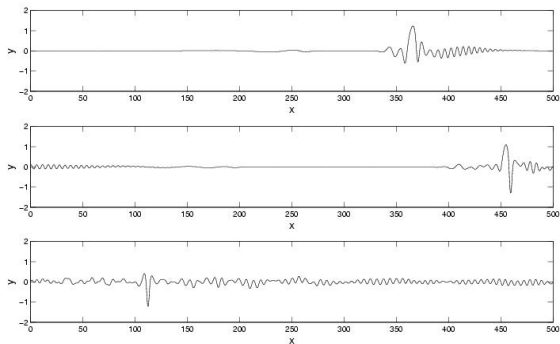
Snapshots of the ice-sheet deflection  $\eta(x, t)$  at  $t = 50, 120, 330, 1000$  (from top to bottom) for  $c = 1.32$

# Numerical results: stability (HOS, $h = \infty$ )



Snapshots of the ice-sheet deflection  $\eta(x, t)$  at  $t = 50, 120, 330, 1000$  (from top to bottom) for  $c = 1.21$

# Numerical results: stability ( $\text{HOS}, h = \infty$ )



Snapshots of the ice-sheet deflection  $\eta(x, t)$  at  $t = 52, 123.5, 325$  (from top to bottom) for  $c = 1.26$

# Energetic consideration (BIE, $h = \infty$ )

These observations on change of stability are consistent with

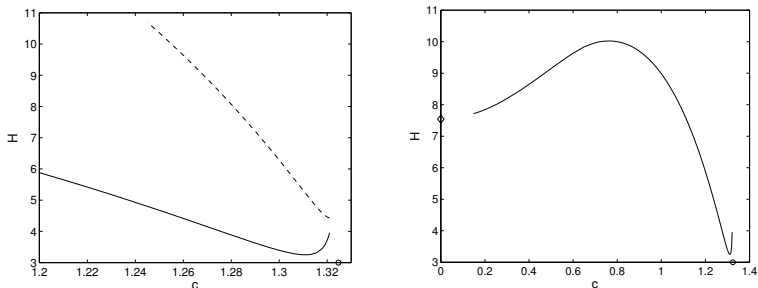


**Figure: Left:** energy for the depression solitary wave branch (solid line) and for the elevation branch (dashed line) for  $1.2 < c < 1.321$ . **Right:** energy of the entire depression solitary wave branch computed up to the limiting case for  $0.15 < c < 1.321$ . The value  $c_{\min}$  is marked by a circle and the energy of the singular solution for  $c = 0$  with self-intersecting profile is marked by  $\diamond$ .

# Weakly nonlinear modeling (modulational regime)

We look for solutions in the form of quasi-monochromatic waves with carrier wavenumber  $k_0 = k_{\min} > 0$  and with slowly varying amplitude depending on  $X = \varepsilon x$  where  $\varepsilon \ll 1$

- Normal mode decomposition

$$\eta \simeq \frac{1}{\sqrt{2}} a^{-1}(D)(z + \bar{z}), \quad \xi \simeq \frac{1}{\sqrt{2}i} a(D)(z - \bar{z})$$

where

$$a(D) = \sqrt[4]{\frac{g + \mathcal{D}D^4/\rho}{G_0}},$$

- Modulational Ansatz

$$z = \varepsilon u(X, t) e^{ik_0 x}, \quad \bar{z} = \varepsilon \bar{u}(X, t) e^{-ik_0 x}$$

# Weakly nonlinear modeling (modulational regime)

- Expansion in  $\varepsilon$  of the Hamiltonian

$$H = \varepsilon \int_{-\infty}^{\infty} \left[ \frac{\bar{u}}{2} \left( \omega(k_0) + \varepsilon \partial_k \omega(k_0) D_X + \frac{\varepsilon^2}{2} \partial_k^2 \omega(k_0) D_X^2 \right) u + \text{c.c.} \right. \\ \left. + \frac{\varepsilon^2}{2} \left( \frac{k_0^3}{2} - \frac{5 \mathcal{D} k_0^7}{4 \rho (g + \mathcal{D} k_0^4 / \rho)} \right) |u|^4 \right] dX + O(\varepsilon^4)$$

where

$$\omega(k) = \sqrt{G_0 (g + \mathcal{D} k^4 / \rho)},$$

denotes the linear dispersion relation in terms of the angular frequency.

- The equations of motion become

$$\partial_t \begin{pmatrix} u \\ \bar{u} \end{pmatrix} = \begin{pmatrix} 0 & -i\varepsilon^{-1} \\ i\varepsilon^{-1} & 0 \end{pmatrix} \begin{pmatrix} \delta H / \delta u \\ \delta H / \delta \bar{u} \end{pmatrix}$$

# Weakly nonlinear modeling ( $k \simeq k_{\min}$ , $h = \infty$ )

Small-amplitude wavepackets satisfy the NLS equation

$$i\partial_\tau u + \lambda \partial_X^2 u + \mu |u|^2 u = 0$$

where  $\tau = \varepsilon^2 t$  and

$$\begin{aligned}\lambda &= \frac{15(\mathcal{D}/\rho)^2}{8(gk_0 + \mathcal{D}k_0^5/\rho)^{3/2}} \left[ k_0^4 + \left( 1 + \frac{4}{\sqrt{15}} \right) \frac{g\rho}{\mathcal{D}} \right] \left[ k_0^4 + \left( 1 - \frac{4}{\sqrt{15}} \right) \frac{g\rho}{\mathcal{D}} \right] \\ &= \frac{15(\mathcal{D}/\rho)^2}{8(gk_0 + \mathcal{D}k_0^5/\rho)^{3/2}} \left[ k_0^4 + \left( 1 + \frac{4}{\sqrt{15}} \right) 3k_{\min}^4 \right] \left[ k_0^4 + \left( 1 - \frac{4}{\sqrt{15}} \right) 3k_{\min}^4 \right] \\ \mu &= \frac{3\mathcal{D}k_0^3/\rho}{4(g + \mathcal{D}k_0^4/\rho)} \left( k_0^4 - \frac{2g\rho}{3\mathcal{D}} \right) = \frac{3\mathcal{D}k_0^3/\rho}{4(g + \mathcal{D}k_0^4/\rho)} (k_0^4 - 2k_{\min}^4)\end{aligned}$$

Here  $\lambda\mu < 0$  for  $k_0 = k_{\min}$  (defocusing), which implies that localized NLS solitons do not exist in this case.

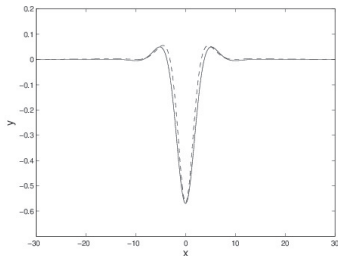
# Weakly nonlinear modeling ( $k \simeq k_{\min}$ , finite depth)

Small-amplitude waves of carrier wavenumber  $k_0$  satisfy a defocusing/focusing NLS equation depending on water depth

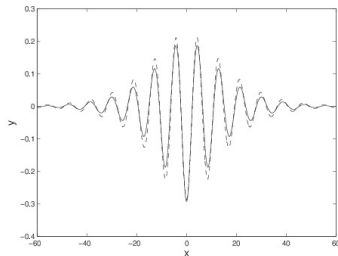
$$i\partial_\tau u + \lambda \partial_X^2 u + \mu |u|^2 u = 0$$

where  $\lambda = \frac{1}{2} \partial_k^2 \omega > 0$  and

$\mu \gtrless 0$  (focusing/defocusing) for  $h \lesseqgtr h_c$



$c = 0.9, h = 1.5$



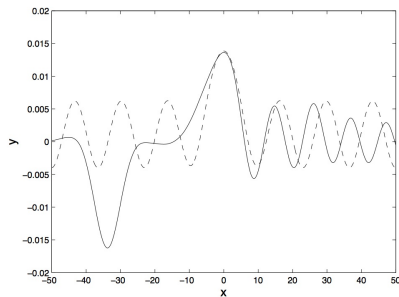
$c = 1.3, h = 3.095$



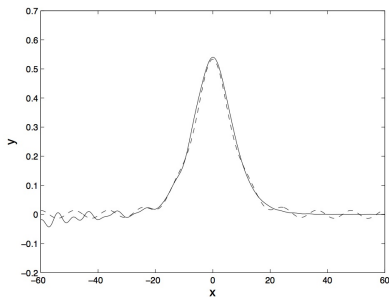
# Weakly nonlinear modeling ( $k \simeq 0$ , shallow water)

Small-amplitude long waves (on shallow water) satisfy a 5th-order KdV equation

$$\partial_{\tau} u + 3c_2 u \partial_X u + c_3 \partial_X^3 u + 2c_4 \partial_X u \partial_X^2 u + c_4 u \partial_X^3 u + c_5 \partial_X^5 u = 0$$



$c = 0.722, h = 0.5$



$c = 1.905, h = 3.095$

## Weakly nonlinear modeling ( $k \simeq 0$ , shallow water)

- Wavelength  $\ell_d = 2\pi/k_d$  of these dispersive tails is determined by the resonance condition

$$c_d(k_d) = \sqrt{h} \left[ 1 - \frac{1}{6} h^2 k_d^2 + \left( \frac{19}{360} h^4 + \frac{1}{2} \right) k_d^4 \right] = c$$

where  $c_d$  is the 5th-order KdV approximation of the linear dispersion relation.

- On which side the dispersive tail appears is determined by the value of its group velocity  $c_g$  relative to that of its phase velocity  $c_p$ . If  $c_g < c_p$ , then the ripples appear behind the solitary pulse. Otherwise, they appear ahead of it.
- Here  $c_g < c_p$  if  $k_d < k_{\min}$  and larger otherwise.
- For  $(c, h) = (0.722, 0.5)$ , we have  $k_d = 0.501 > k_{\min} = 0.204$ , so ripples are ahead (right side). For  $(c, h) = (1.905, 3.095)$ , we have  $k_d = 0.586 < k_{\min} = 0.735$ , so ripples are behind (left side).

# Conclusions

- Hamiltonian formulation for fully nonlinear ice-covered ocean waves
- Direct numerical simulations
- Weakly nonlinear models in the modulational and long-wave limits
- Small-amplitude solitary waves of depression are unstable
- Large-amplitude solitary waves of depression are stable
- Solitary waves of elevation are unstable